Thermal conductivity of the Lennard-Jones chain fluid model

Guillaume Galliero* and Christian Boned
Laboratoire des Fluides Complexes (UMR-5150, CNRS and TOTAL), Université de Pau et des Pays de l'Adour, BP 1155, F-64013 Pau Cedex, France

(Received 18 September 2009; revised manuscript received 4 November 2009; published 10 December 2009)

Nonequilibrium molecular dynamics simulations have been performed to estimate, analyze, and correlate the thermal conductivity of a fluid composed of short Lennard-Jones chains (up to 16 segments) over a large range of thermodynamic conditions. It is shown that the dilute gas contribution to the thermal conductivity decreases when the chain length increases for a given temperature. In dense states, simulation results indicate that the residual thermal conductivity of the monomer increases strongly with density, but is weakly dependent on the temperature. Compared to the monomer value, it has been noted that the residual thermal conductivity of the chain was slightly decreasing with its length. Using these results, an empirical relation, including a contribution due to the critical enhancement, is proposed to provide an accurate estimation of the thermal conductivity of the Lennard-Jones chain fluid model (up to 16 segments) over the domain $0.8 \leq T^* \leq 6$ and $0 \leq \rho^* \leq 1$. Additionally, it has been noted that all reduced thermal conductivity values of the Lennard-Jones chain fluid model merge on the same "universal" curve when plotted as a function of the excess entropy. Furthermore, it is shown that the reduced configurational thermal conductivity of the Lennard-Jones chain fluid model is approximately proportional to the reduced excess entropy for all fluid states and all chain lengths.

DOI: 10.1103/PhysRevE.80.061202 PACS number(s): 65.20.De, 66.10.cd, 02.70.Ns

I. INTRODUCTION

Kinetic theories [1] provide accurate estimation of transport properties of atomic fluids in the low density regime. Nevertheless, the situation is more complex when dealing with dense and/or molecular fluids, especially for thermal conductivity [2,3]. In fact, no rigorous theory is yet available for an exact estimation of transport properties in dense fluids in terms of interaction potentials and molecular description [2]. Concerning mass diffusion and viscosity, which are closely related properties, there exist recent attempts to construct theories/correlations dedicated to various molecular models, from the hard-sphere to Lennard-Jones chain e.g., [4–13]. However, less work has been dedicated to the thermal conductivity of these molecular models in dense fluid states [2,6,8,14–16]. Among them, the approach of Assael *et al.* [2,14] based on the rough hard-sphere model is able to provide an excellent estimation of the thermal conductivity of various pure fluids and mixtures of compounds belonging to the same class, but is sometimes not as precise on asymmetric mixtures containing different classes of compounds [2]. Concerning the approach based on the Lennard-Jones fluid model [15,16], which is generally a suitable fluid model for viscosity prediction [9], it is efficient to predict the thermal conductivity of atomic fluids but is inadequate when dealing with molecular fluids [16].

Using extensive molecular dynamics (MD) simulations, we have performed a systematic study of the thermal conductivity of the Lennard-Jones chain (LJC) model in various fluid states (gas, liquid, supercritical). In such model, the molecule is described by a chain of freely jointed spheres and nonbonded interactions are described by a Lennard-Jones (LJ) potential. The simulations have been performed on short chains composed of 1, 2, 4, 8, and 16 spheres for a wide range of thermodynamic states covering gas, liquid and supercritical conditions. A nonequilibrium molecular dynamics (NEMD) scheme has been employed to compute the thermal conductivity.

Starting from the simulation results, several features of the thermal conductivity of the LJ and of the LJC fluids are discussed in this work. The three contributions to the thermal conductivity (dilute gas, critical and residual) have been quantified and correlated. The influence on thermal conductivity of the internal degrees of freedom induced by the chain description have been analyzed and modeled for all fluid states. Finally, the expected link between the thermal conductivity and the excess entropy [17,18] has been studied for the monomer and the chains.

II. MODEL AND THEORY

A. Molecular model

To describe the fluid particles, we employ in this work the Lennard-Jones chain fluid model (homonuclear) with rigid bonds. Each LJC molecule is modeled as a set of N tangent spheres (segments), freely jointed, with bond lengths constrained. In this work, we have considered molecules composed of 1, 2, 4, 8, and 16 spheres, i.e., short chains.

Intermolecular and nonbonded intramolecular interactions of nonadjacent spheres are described by the truncated Lennard-Jones 12–6 potential:

$$u = \begin{cases} 4\left[\left(\frac{\sigma}{r}\right)^{12} - \left(\frac{\sigma}{r}\right)^{6}\right] & \text{if } r \leq r_c \\ 0 & \text{if } r > r_c \end{cases}, \tag{1}$$

where ε is the potential strength, σ, the segment diameter, which is the distance at which the potential is null, r the

*Corresponding author. FAX: +33 5 59 40 7695; guillaume.galliero@univ-pau.fr

distance between the considered segments. The cut off radius, r_c, has been taken equal to 2.5σ [15]. In order to maintain the bond length between adjacent segments equal to σ, we have employed the classical RATTLE algorithm [19]. It is worth to mention that the use of a constrained bonds limit the number of internal degrees of freedom compared to a model with flexible bonds and so simplify the analysis.

For sake of generality, all variables are expressed in dimensionless units, noted with a star as superscript. The scaling has been done using the molecular parameters of the monomer, i.e., σ, ε, and M, where M is the mass of the monomer. Using that set of parameters, dimensionless temperature, T^*, density, ρ^*, and thermal conductivity, λ^*, are expressed as:

$$T^* = \frac{k_B T}{\varepsilon}, \quad \rho^* = \frac{N_S \sigma^3}{V} \quad \text{and} \quad \lambda^* = \lambda \frac{\sigma^2}{k_B} \left(\frac{M}{\varepsilon} \right)^{1/2}, \quad (2)$$

where k_B is the Boltzmann constant, N_S the total number of spheres/segments inside the simulation box (i.e., $N \times N_{mol}$, where N_{mol} is the number of molecules and N the number of segments of a chain) and V the volume of the simulation box.

B. Non Equilibrium Molecular Dynamics algorithm

To compute the thermal conductivity from MD simulations, we have employed a boundary driven NEMD, compatible with periodic boundary conditions. The approach chosen in this work has been first proposed by Müller-Plathe [20] for monoatomic fluids and then extended by Bedrov *et al.* [21] to be applicable to molecular fluids with internal constraints like the LJC fluid model employed in this work. In order to ensure the consistency of the approach, we have compared some of the results on thermal conductivity obtained by this NEMD scheme with those computed using another algorithm proposed previously by Hafskjold *et al.* [22]. In all cases, results obtained by the two schemes were consistent with each other, i.e., thermal conductivity values using both schemes were within error bars. In this article, only the results obtained by the Müller-Plathe/Bedrov NEMD approach are provided.

To compute the thermal conductivity using this NEMD scheme, the simulation box is divided in n_s slabs along the z direction. Then, are selected the two molecules in slabs 1 and n_s with the highest kinetic energy (the "hottest" molecules) and the two molecules in slabs $n_s/2$ and $n_s/2+1$ with the lowest kinetic energy (the "coldest" molecules). Finally, the translational velocities of these molecules are exchanged between the central part of the simulation box and the edge layers. This procedure keeps constant the overall energy and linear momentum and corresponds to a redistribution of a certain amount of kinetic energy, ΔE_c^*, in the simulation box [21]. This exchange is done every A time steps (the exchange frequency). It corresponds to an imposed heat flux, $\mathbf{J}_q^*$, along the direction z:

$$(\mathbf{J}_q^*)_z = \frac{\Delta E_c^*}{2A \delta t^* L_x^* L_y^*}, \quad (3)$$

where δt^* is the time step and L_x^*, L_y^* are the lengths of the simulation box, respectively, in the x and y directions.

Once the stationary state is reached, the thermal conductivity in pure fluids is simply deduced from the Fourier's law

$$\mathbf{J}_q^* = -\lambda^* \nabla T^* \quad (4)$$

and the measured biperiodical temperature profiles. The slabs where the exchanges are performed, as well as their first neighbors, have been discarded to measure the temperature gradients [23].

C. Numerical details

Computations have been performed with a homemade code already validated in previous works [13,16]. To integrate the equation of motion with the constraint on the bond length, the RATTLE algorithm is used [19]. A dimensionless time step, $\delta t^* = 0.003$ has been employed. Periodic boundary conditions combined with a Verlet neighbors list have been applied [24]. To maintain the averaged temperature during the simulations, a Berendsen thermostat has been used [25] with a large time constant equal to $1000 \delta t^*$.

The system was set up by placing N_{mol} molecules in a parallelipipedic simulation box elongated in the direction of the thermal gradient with $L_x^* = L_y^* = L_z^*/2$, except for $\rho^* = 0.1$ for which $L_x^* = L_y^* = L_z^*/4$. The number of molecules, N_{mol}, was fixed to 3000 for $N=1$, 1500 for $N=2$, 750 for $N=4$, 375 for $N=8$, and 250 for $N=16$. These values ensure to avoid noticeable finite size effects (see following section). During NEMD simulations, the exchange frequency, A, was selected so that the relative temperature difference $(T_{hot} - T_{cold})/T_{average}$ was always smaller than 0.2 to avoid non linear response, i.e., A was varying from 70 (dense state for a monomer) to 850 (dilute state for an octomer). After having reached the stationary state, each run has been performed during at least 10^7 nonequilibrium time steps to obtain the thermal conductivity. In order to estimate errors on the computed variables, the sub-blocks average method has been applied [24].

III. RESULTS

A. Preliminary results

Contrary to our previous work on the Lennard-Jones fluid model [16], the simulation box employed in this work is elongated along the direction of the thermal gradient, cf. previous section. By using such a noncubic simulation box, the influence of the number of particles employed on the thermal conductivity was found to be negligible for simulations using more than 1000 LJ spheres as shown on Fig. 1 for the monomer. This weak size dependence in both dense ($T^*=2$, $\rho^*=0.8$) and dilute states ($T^*=4$, $\rho^*=0.2$) is consistent with the literature [23,26]. A similar weak size dependence (above roughly 1000 spheres) has been noticed for N-mer systems.

B. Dilute gas contribution

It is usually assumed that thermal conductivity of fluids may be written as the sum of three terms [2]:

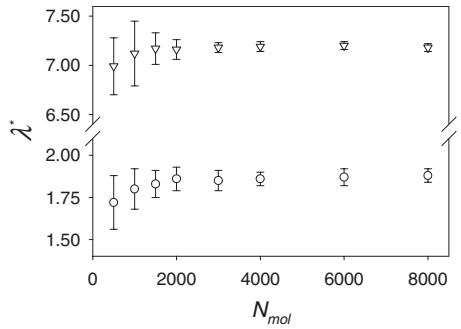

FIG. 1. Influence of the number of molecules used on computed thermal conductivity for the monomer in two very different states, $T^*=4$, $\rho^*=0.2$ (circles), and $T^*=2$, $\rho^*=0.8$ (down triangles).

$$\lambda = \lambda_0 + \lambda_r + \lambda_c, \tag{5}$$

where λ_0, is the dilute gas contribution, λ_r the residual thermal conductivity and λ_c the critical enhancement appearing in the vicinity of the critical point.

In the simple Lennard-Jones case (monomer), for which only translational transport of energy occurs, the dilute gas contribution to the thermal conductivity can be estimated using the first order Chapman-Enskog [1,2] solution to the Boltzmann equation:

$$\lambda^*_{0,LJ} = \frac{75}{64\Omega_v}\sqrt{\frac{T^*}{\pi}}, \tag{6}$$

where Ω_v is the collision integral that can be estimated using the correlation proposed by Neufeld *et al.* [27], which is valid for T^* varying from 0.3 to 100.

The problem is by far more complex in a polyatomic system, for which a molecule may store energy in forms other than translational. There is no exact solution to that problem, even for the LJC fluid model, and several approximations have been proposed that couple, or not, contributions due to translational and internal degrees of freedom [2,3]. As already done for the LJC viscosity [13], one way to provide information on the dilute gas thermal conductivity of the LJC is to deduce it directly from NEMD simulations at low density. To do so, we take advantage of the fact that it exists a microscopic formulation of the heat flux of molecular fluids [28,29] that can be estimated during MD simulations. In that frame, the instantaneous microscopic heat flux can be written as the sum of two terms [30,31]:

$$\mathbf{J}_q{}^* = \mathbf{J}_{q,k}{}^* + \mathbf{J}_{q,p}{}^* \tag{7}$$

where $\mathbf{J}_{q,k}{}^*$ and $\mathbf{J}_{q,p}{}^*$ represents, respectively, the kinetic (or translational) and the potential (or configurational) contributions to the heat flux. For a LJC fluid, the kinetic contribution can be written as [28,29]

$$\mathbf{J}_{q,k}{}^* = \frac{1}{V^*}\sum_a \left\{ \frac{1}{2}\sum_{i\in a} (\mathbf{v}_i^*)^2 \mathbf{v}_a{}^* \right\} \tag{8}$$

and the potential contribution as

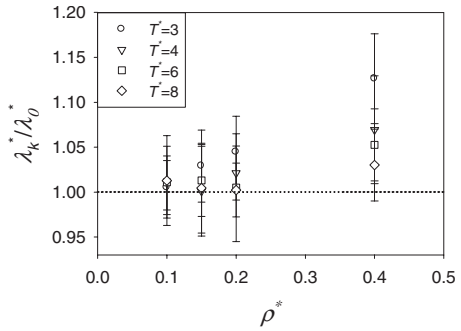

FIG. 2. Ratio between the kinetic thermal conductivity computed using NEMD simulations and the dilute gas thermal conductivity estimated using Eq. (6) for a LJ fluid model and for various thermodynamic conditions.

$$\mathbf{J}_{q,p}{}^* = \frac{1}{V^*}\sum_a \left\{ \left[\sum_{i,j\in a} u_{ij}{}^* + \frac{1}{2}\sum_{i\in a}\sum_{b\neq a}\sum_{j\in b} u_{ij}{}^* \right] \mathbf{v}_a{}^* - \frac{1}{2}\sum_{i\in a}\sum_{b\neq a}\sum_{j\in a} \mathbf{r}_{ab}{}^* \times [\mathbf{F}_{ij}{}^* \cdot \mathbf{v}_i^*] \right\}, \tag{9}$$

where a and b are molecular indices and i and j are atomic indices. $\mathbf{v}$ is the velocity vector (all velocities are barycentric), $\mathbf{r}$ is the position vector and $\mathbf{F}$ the Lennard-Jones force. Using that decomposition and Eq. (4), it follows that the thermal conductivity is composed of two terms:

$$\lambda = \lambda_k + \lambda_p, \tag{10}$$

where λ_k and λ_p are respectively the "kinetic" and "potential" contributions to the thermal conductivity. Thus, it is possible to deduce both λ_k and λ_p by computing the microscopic contributions to the heat flux during the NEMD simulations. To ensure the consistency of the approach, it has been verified that the total microscopic heat flux, Eq. (7), is effectively equal (within 2%) to the one imposed by the NEMD scheme employed, Eq. (3).

By definition, it is expected that the kinetic thermal conductivity will tend to the dilute gas value of the thermal conductivity when ρ^* will tend toward zero. So, for various low density conditions, we have computed the $\lambda_k{}^*$ of the LJ fluid model (monomer) to compare it with the dilute gas value, $\lambda_0{}^*$, calculated using Eq. (6).

Interestingly, Fig. 2 shows that, for a given temperature, the kinetic thermal conductivity slightly increases with density and more important is very close to its dilute gas value for sufficiently low-density simulations. As an example, the absolute deviation between $\lambda_k{}^*$ at $\rho^*=0.1$ and $\lambda_0{}^*$ is of the order of 1% whatever the temperature. More generally, when the kinetic thermal conductivity represents more than 70% of the total thermal conductivity, it has been found that its value does not exceed from more than 5% the dilute gas one. Thus, the computation of $\lambda_k{}^*$ provides a very good approximation of $\lambda_0{}^*$ for the monoatomic LJ fluid for sufficiently dilute conditions, i.e., when $\lambda_k{}^*/\lambda^*$ is greater than 70%.

So, assuming that such behavior remains valid whatever N, we have computed $\lambda_k{}^*$ at $\rho^*=0.1$ (verifying that in all simulated cases $\lambda_k{}^*/\lambda^* > 70\%$) for $N=2$, 4, and 8 and vari-

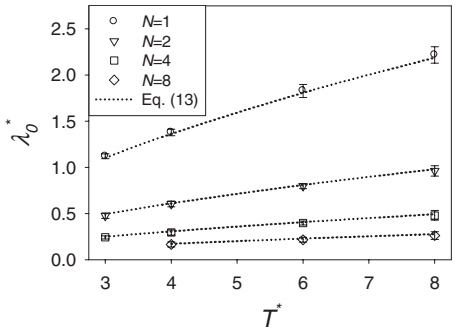

FIG. 3. Dilute gas thermal conductivity of the LJC fluids computed from NEMD simulations and estimated from the proposed relation, Eq. (13).

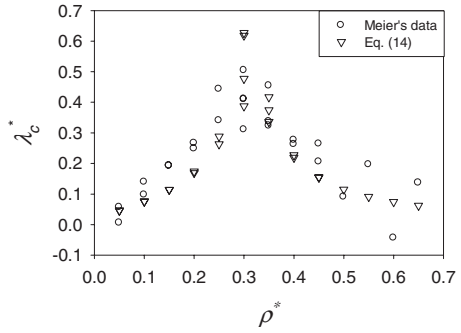

FIG. 4. Critical enhancement contribution to the thermal conductivity of the LJ fluid model. Different points for a given density correspond to slight variations on the temperature around $T^*=1.35$ [31].

ous T^* to provide an estimate of the dilute gas thermal conductivity of the LJC fluid for different values of N. It should be noted that the case, for which $N=16$ has not been included in this part of the discussion because of a too small signal to noise ratio (i.e., a large exchange frequency).

As expected, Fig. 3 clearly exhibits that, λ_0^* of the LJC fluid decreases with chain length for a given T^*. In addition λ_0^* increases with T^* whatever the chain length. Both behaviors are consistent with those of simple real linear molecules such as normal alkanes at low density.

In order to relate the λ_0^* values obtained for polymer ($N>1$) to that of the monomer, we have started from the well known relation proposed by Eucken [3], which, for a LJC fluid model, writes simply as:

$$\frac{\lambda^* N}{\eta^* C_V^*} = 1 + \frac{9}{4C_V^*}, \tag{11}$$

where C_V^* is the constant volume heat capacity and η^* the shear viscosity. It should be noted that such relations relies on the assumption that translational and internal degrees of freedom are considered to be decoupled. In a previous work [13], we have shown that the dilute gas viscosity of the LJC fluid is simply equal to that of the monomer divided by the square root of the number of segment, $\eta_{0,LJC}^* = \eta_{0,LJ}^*/N^{1/2}$. So, using the fact that at dilute gas conditions $C_V^* = (2N+1)/2$ for a LJC fluid, one can deduce from Eq. (11) a relation for the dilute gas thermal conductivity of the LJC fluid, $\lambda_{0,LJC}^*$, relatively to that of the monomer, $\lambda_{0,LJ}^*$:

$$\frac{\lambda_{0,LJC}^*}{\lambda_{0,LJ}^*} = \frac{4N+11}{15N^{3/2}} \tag{12}$$

and using Eq. (6) we get:

$$\lambda_{0,LJC}^* = \frac{5(4N+11)}{64N^{3/2}\Omega_v}\sqrt{\frac{T^*}{\pi}} \tag{13}$$

It is worth noting that this relation ensures that $\lambda_{0,LJC}^*(N=1) = \lambda_{0,LJ}^*$.

As clearly shown on Fig. 3, Eq. (13) is able to provide an excellent estimation of the dilute gas thermal conductivity of the LJC fluid, whatever the length of the chain N. The average absolute deviation (AAD) between $\lambda_{0,LJC}^*$ calculated using Eq. (13) and those obtained by NEMD simulations is equal to 3.2% with a maximum deviation (MxD) of 6.1%.

C. Critical enhancement

Close to the critical point, the thermal conductivity diverges following a scaling law [32]. This induces a non negligible enhancement of the thermal conductivity even not very close to the critical point. Such an enhancement has been noticed using molecular dynamics simulations, even if MD results are scarce [16,31,33]. Nevertheless, in molecular simulations, this enhancement due to long-range correlations could not properly be taken into account because of the finite size of the system simulated. In addition, NEMD simulations imply the use of a not too small temperature gradient, which induces further problems to catch properly the critical enhancement [16].

So, in order to roughly quantify the influence of the critical point of the thermal conductivity, we have employed simulations data coming from equilibrium molecular dynamics (EMD) provided by Meier [31]. These simulations have been performed on the Lennard-Jones fluid model (monomer), with a cutoff radius of 5σ, for a temperature very close to the critical one, $T^*=1.35\pm0.01$. From these data, we have deduced λ_c^*, using $\lambda_c^* = \lambda^* - (\lambda_0^* + \lambda_r^*)$. To calculate λ_0^*, we have employed Eq. (6), and to estimate λ_r^*, we have employed the scheme that is presented in the following section.

As expected, Fig. 4 shows that λ_c^* of the LJ fluid at $T^*=1.35\pm0.01$ increases with ρ^* up to $\rho^*\sim0.3$ and then decreases. For the studied states, λ_c^* contributes up to 30% of the total thermal conductivity, which is by far not negligible. To represent approximately this contribution in a very simple manner, we have assumed, following [16,34], that the critical contribution to the thermal conductivity of the LJC fluid can be approximated by:

$$\lambda_c^* = a_1\left(\frac{\rho^{*2}\beta_T^*}{T^*}\right)^{a_2}, \tag{14}$$

where β_T^* is the isothermal compressibility and the a_i are numerical parameters fitted on the EMD data of Meier [31].

In order to compute the isothermal compressibility for the monomer (which diverges close to the critical point), we

TABLE I. Thermal conductivity, λ^*, of the LJC fluid computed by NEMD simulations.

T^*	ρ^*	$N=1$	$N=2$	$N=4$	$N=8$	$N=16$
2	1	12.74 ± 0.28	10.37 ± 0.25	9.5 ± 0.15	8.84 ± 0.31	8.65 ± 0.34
3	1	13.5 ± 0.24	11.18 ± 0.21	10.03 ± 0.24	9.55 ± 0.29	9.3 ± 0.29
4	1	14.03 ± 0.27	11.66 ± 0.21	10.47 ± 0.21	9.85 ± 0.29	9.73 ± 0.29
6	1	14.78 ± 0.45	12.28 ± 0.4	10.91 ± 0.41	10.63 ± 0.45	10.35 ± 0.4
0.8	0.9	8.33 ± 0.14	6.68 ± 0.12	5.89 ± 0.14	5.41 ± 0.12	5.3 ± 0.15
0.9	0.9	8.49 ± 0.16	6.78 ± 0.15	5.96 ± 0.15	5.61 ± 0.11	5.45 ± 0.16
1	0.9	8.68 ± 0.14	6.92 ± 0.11	6.1 ± 0.12	5.73 ± 0.13	5.6 ± 0.21
1.5	0.9	9.32 ± 0.18	7.47 ± 0.15	6.6 ± 0.14	6.29 ± 0.14	6.04 ± 0.14
2	0.9	9.75 ± 0.16	7.76 ± 0.17	6.93 ± 0.12	6.48 ± 0.24	6.31 ± 0.23
3	0.9	10.45 ± 0.15	8.54 ± 0.18	7.44 ± 0.19	6.93 ± 0.23	6.82 ± 0.25
4	0.9	10.79 ± 0.18	8.77 ± 0.25	7.64 ± 0.25	7.36 ± 0.32	7.13 ± 0.18
6	0.9	11.31 ± 0.27	9.36 ± 0.26	8.31 ± 0.21	7.87 ± 0.21	7.55 ± 0.29
1	0.8	6.33 ± 0.1				
1.5	0.8	6.77 ± 0.09	5.38 ± 0.11	4.56 ± 0.09	4.25 ± 0.11	4.02 ± 0.09
2	0.8	7.18 ± 0.05	5.66 ± 0.09	4.89 ± 0.08	4.56 ± 0.16	4.4 ± 0.17
3	0.8	7.74 ± 0.21	6.05 ± 0.15	5.38 ± 0.18	4.85 ± 0.17	4.65 ± 0.26
4	0.8	8.19 ± 0.11	6.48 ± 0.23	5.59 ± 0.21	5.11 ± 0.15	4.96 ± 0.23
6	0.8	8.81 ± 0.17				
1.5	0.6	3.51 ± 0.05				
2	0.6	3.77 ± 0.07	2.79 ± 0.16	2.29 ± 0.07		
3	0.6	4.25 ± 0.12	3.11 ± 0.14	2.47 ± 0.15	2.29 ± 0.12	2.18 ± 0.08
4	0.6	4.7 ± 0.15	3.39 ± 0.17	2.74 ± 0.1	2.51 ± 0.17	2.4 ± 0.09
6	0.6	5.36 ± 0.12				
1.5	0.4	1.92 ± 0.05				
2	0.4	2.13 ± 0.07	1.35 ± 0.04			
3	0.4	2.48 ± 0.07	1.56 ± 0.09	1.14 ± 0.1	0.97 ± 0.05	0.92 ± 0.04
4	0.4	2.82 ± 0.06	1.73 ± 0.08	1.23 ± 0.06	1.06 ± 0.09	1.02 ± 0.04
6	0.4	3.4 ± 0.1				
2	0.2	1.25 ± 0.03				
3	0.2	1.56 ± 0.05	0.82 ± 0.02	0.506 ± 0.021	0.359 ± 0.018	
4	0.2	1.84 ± 0.04	0.94 ± 0.03	0.557 ± 0.027	0.394 ± 0.025	
6	0.2	2.32 ± 0.1	1.18 ± 0.07	0.684 ± 0.013	0.467 ± 0.032	
3	0.1	1.3 ± 0.03	0.583 ± 0.036	0.324 ± 0.024		
4	0.1	1.58 ± 0.04	0.721 ± 0.037	0.378 ± 0.035	0.231 ± 0.04	
6	0.1	2.07 ± 0.08	0.932 ± 0.033	0.492 ± 0.026	0.287 ± 0.035	
8	0.1	2.48 ± 0.1	1.113 ± 0.066	0.586 ± 0.064	0.345 ± 0.054	

have employed the accurate Lennard-Jones equation of state (EoS) of Kolafa and Nezbeda [35]. This EoS predicts a critical point located at $\rho_c^*=0.3108$ and $T_c^*=1.3396$, these values being consistent with the position of the critical point of the LJ fluid with a cutoff radius of 5σ employed by Meier [36]. In addition, to compute β_T^* for chains, we have employed the chain term developed by Johnson *et al.* [37] combined with the EoS of Kolafa and Nezbeda [35] for the LJ reference term. This equation of state is sometimes called LJ-SAFT (statistical associating fluid theory) in the literature.

As shown on Fig. 4, Eq. (14) is able to correctly represent the critical enhancement, λ_c^*, of the monomer using $a_1=0.2$ and $a_2=0.45$ despite the simplicity of the approach. The value of a_2 is taken positive, which ensures that in the ideal gas limit, λ_c^* tends to zero. It should be noted that we have used a 2.5σ cutoff radius, which implies a critical temperature lower than the one for a full LJ potential [36]. This surely imply a slight discrepancy between the value of λ_c^* deduced from the EoS scheme and the one corresponding to our simulations with $r_c^*=2.5$.

D. Residual contributions

1. Monomer term

In order to quantify the residual thermal conductivity, λ_r^*, cf. Eq. (5), we have computed the thermal conductivity, λ^*,

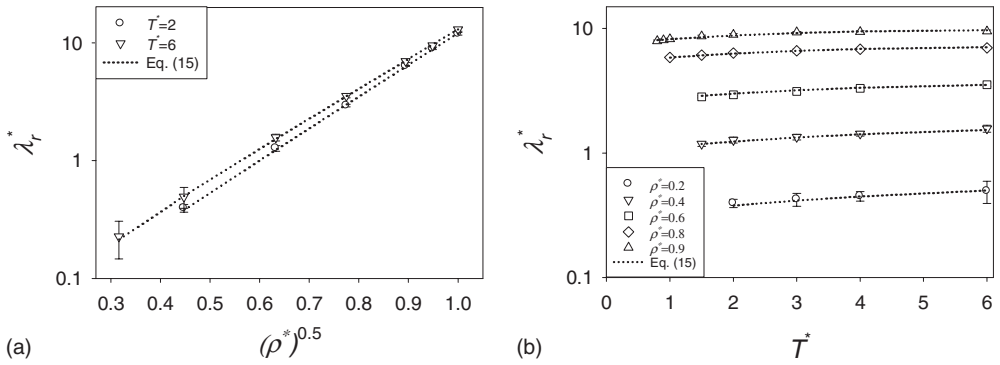

FIG. 5. Residual thermal conductivity of the LJ fluid model (monomer) for different thermodynamic conditions.

of the LJ fluid model using the non-cubic simulation box. These NEMD computations on the monomer have been performed for a wide range of thermodynamic conditions, i.e., ρ^* varying from 0.1 to 1 and T^* ranging from 0.8 to 8. All simulation results are provided in Table I.

From these simulations data, we have deduced λ_r^* using $\lambda_r^* = \lambda^* - (\lambda_0^* + \lambda_c^*)$. To calculate λ_0^*, we have employed Eq. (6), and to estimate λ_c^*, we have used Eq. (14). In a first step, to perform the analysis, we have discarded the critical point region so that the critical enhancement, λ_c^*, was always below 5% of the total thermal conductivity value.

Fig. 5 clearly shows that the residual thermal conductivity of the monomer increases strongly with density in a rather simple manner, i.e., $\ln(\lambda_r^*) \propto (\rho^*)^{1/2}$, for the whole range of ρ^* studied here. In addition, one can notice a weak, but non negligible, non linear effect of temperature on λ_r^*, the larger the temperature the bigger λ_r^*, see Fig. 5.

So, using these results, we have checked that the residual thermal conductivity of the LJ fluid (monomer) can be well correlated by:

$$\lambda_{r,LJ}^* = (b_1 + b_2 T^*)[e^{(b_3 + b_4 T^*)\sqrt{\rho^*}} - 1], \tag{15}$$

where the b_i are numerical parameters that have been adjusted on NEMD data. The optimal values of these numerical parameters are given in Table II. As shown on Fig. 5, Eq. (15) is able to represent accurately (within the error bars) the residual thermal conductivity of the monomer whatever the state.

Thus, if all three contributions to thermal conductivity of the LJ fluid are gathered together, Eqs. (6), (14), and (15), one can write that the thermal conductivity of the LJ fluid (monomer) can be represented by:

$$\lambda_{LJ}^* = \frac{75}{64\Omega_v}\sqrt{\frac{T^*}{\pi}} + a_1\left(\frac{\rho^{*2}\beta_T^*}{T^*}\right)^{a_2} + (b_1 + b_2 T^*)[e^{(b_3 + b_4 T^*)\sqrt{\rho^*}} - 1]. \tag{16}$$

TABLE II. Numerical parameters of Eq. (15) adjusted on the NEMD.

b_1	b_2	b_3	b_4
0.01827376	0.00384599	6.33482906	−0.09646083

This correlation is able to provide an excellent estimation of the thermal conductivity of the Lennard-Jones fluid. Compared to our NEMD simulation results (36 points) provided in Table I, Eq. (16) yields an AAD=0.87% with a MxD=1.75%. In addition, when applying this correlation to the EMD data of Nasrabad *et al.* [15] (64 points), which covers from $T^*=0.9$ to $T^*=2$ and from $\rho^*=0.3$ to $\rho^*=0.9$, the AAD=2.3% with a MxD=7.3%, which is good, taking into account uncertainties on the MD data.

2. Chain term

In order to analyze the dependence of the residual thermal conductivity with the length of the chain, we have performed NEMD simulations on Lennard-Jones chains of various lengths, $N=2$, 4, 8, and 16. This study has been restricted to short chains so that the dynamic behavior remains in the Rouse regime. The range of stable thermodynamic states tested is the same than for the simulations on the monomer, i.e., T^* varying from 0.8 to 8 and ρ^* varying from 0.1 to 1. This corresponds to 103 points of simulations. All thermal conductivity values obtained by NEMD simulations are provided in Table I.

Results shown on Fig. 6 indicate that $\lambda_{r,LJC}^*$ slightly decreases with the chain length, this behavior being noticed for all studied states. It should be pointed out that the influence of the chain length is rather weak, e.g., $\lambda_{r,LJC}^*$ values for $N=16$ are only ~30% smaller than those of the monomer for a given set of T^* and ρ^*. This is consistent with some experimental results on heavy normal alkane [38], which exhibit a

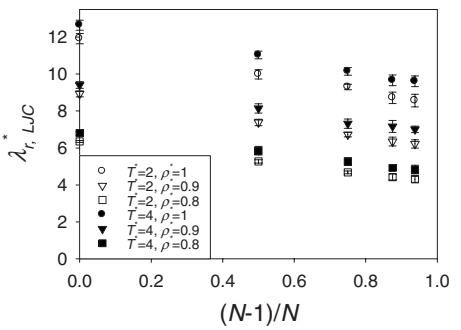

FIG. 6. Residual thermal conductivity of the Lennard-Jones chain fluid model for various chain lengths and different dense thermodynamic states.

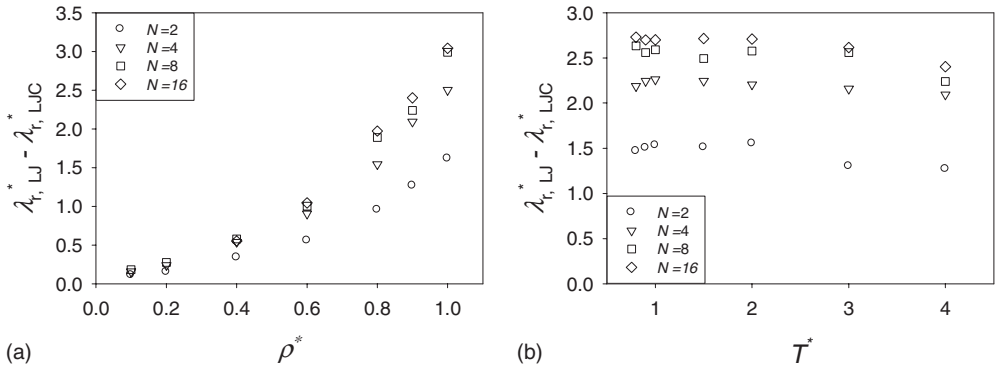

FIG. 7. Residual thermal conductivity of the LJC fluid model for various thermodynamic conditions. Left figure: $T^*=4$. Right figure: $\rho^*=0.9$.

small impact of the chain length on the thermal conductivity amplitude. This decrease is consistent with the fact that increasing the chain length increases the number of internal degrees of freedom. Thus, the longer the chain, the smaller the amount of energy available for heat transport. Another interesting feature shown on Fig. 6 is that the decrease of $\lambda_{r,LJC}{}^*$ is roughly proportional to $(N-1)/N$.

Fig. 7 indicates that the influence of the chain length on the residual thermal conductivity is strongly dependent to the density but only weakly on temperature. It should be noticed that the trends are similar for the states not shown on Fig. 7.

Using the behaviors noted on Figs. 6 and 7, the chain term of the residual thermal conductivity has been written as:

$$\lambda_{r,LJC}{}^* = \lambda_{r,LJ}{}^* - \frac{N-1}{N}[c_1\sqrt{\rho^*}(1+c_2\rho^{*2})], \tag{17}$$

where the c_i are numerical parameters adjusted on our NEMD data (103 points). The best fit yields $c_1=0.572$ and $c_2=4.96$.

Thus, if all contributions are combined together, Eqs. (13)–(15) and (17), our correlation to estimate the thermal conductivity of the LJC fluid model writes as:

$$\lambda_{LJC}{}^* = \frac{5(4N+11)}{64N^{3/2}\Omega_v}\sqrt{\frac{T^*}{\pi}} + a_1\left(\frac{\rho^{*2}\beta_T{}^*}{T^*}\right)^{a_2} + (b_1+b_2T^*) \times[e^{(b_3+b_4T^*)\sqrt{\rho^*}}-1] - \frac{N-1}{N}[c_1\sqrt{\rho^*}(1+c_2\rho^{*2})] \tag{18}$$

This correlation is able to provide an accurate estimation of the thermal conductivity of the Lennard-Jones chain fluid model (up to 16 segments) for a wide range of thermodynamic states when compared to the full set of NEMD data, as indicated in Table III. Interestingly, the quality of the results provided by the correlation remains acceptable when the chain length increases.

TABLE III. Deviations between thermal conduction values provided by Eq. (18) and those obtained by NEMD simulations for the whole range of thermodynamic conditions studied in this work.

	$N=1$	$N=2$	$N=4$	$N=8$	$N=16$
AAD	0.87%	1.35%	1.79%	2.68%	2.45%
MxD	1.75%	4.18%	4.37%	6.70%	6.75%

E. Excess entropy scaling

1. Usual approach

More than thirty years ago, Rosenfeld [17] has shown that for simple atomic fluids, a reduced (suitably scaled) transport property in dense fluids can be directly related to the excess (i.e., configurational) entropy, S^e. This excess entropy is defined as the difference between the thermodynamic entropy and the entropy of the ideal gas at the same conditions [17]. Relations based on similar concept have led to semiquantitative predictions of transport properties of various model and real fluids [18,39–43].

In that frame, the reduced thermal conductivity, λ^r, is defined as [40]:

$$\lambda^r = \lambda\frac{d^2}{k_B^{3/2}}\sqrt{\frac{m}{T}}, \tag{19}$$

where d is the interparticle distance ($d=(V/N_p)^{1/3}$ with N_p the number of particles) and m the mass of the particle. Using results of MD simulations on spheres interacting with various pair potentials, Rosenfeld [40] has found that the reduced thermal conductivity, as function of the reduced excess entropy, $S^r=S^e/(k_BN_p)$, shows a quasi universal behavior of the type:

$$\lambda^r = 1.5e^{-0.5S^r}. \tag{20}$$

In order to test such a relation on the Lennard-Jones chain fluid model, we need to estimate the excess entropy of this model. To do so, we have employed the equation of state described previously, the LJ-SAFT, i.e., a reference LJ term modeled by the Kolafa and Nezbeda EoS [35] and the chain term of Johnson *et al.* [37].

As clearly shown on Fig. 8, the scaling proposed by Rosenfeld is consistent with our NEMD results on the monomer, except in the low density fluid domain when $S^r>-1$ in agreement with previous findings [40]. Within the dense fluid domain, relation Eq. (20) provides values of LJ thermal conductivities that deviates not more than 25% from those computed by NEMD simulations. Nevertheless, Fig. 8 clearly

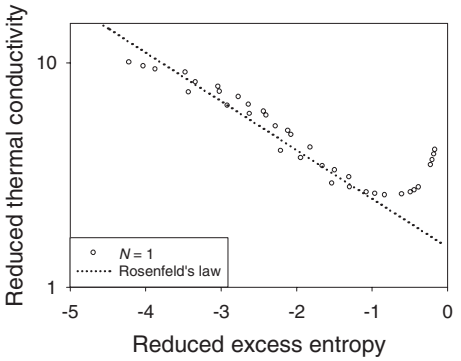

FIG. 8. Reduced thermal conductivity of the LJ monomer computed by NEMD plotted against reduced excess entropy calculated by a LJ EoS.

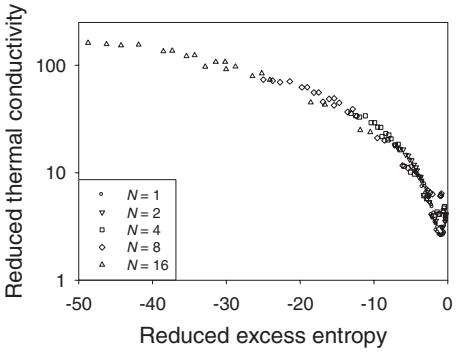

FIG. 9. Reduced thermal conductivity of the LJC fluid model for various chain lengths plotted against reduced excess entropy.

exhibit an inconsistency of such a scaling when the reduced excess entropy tends to zero.

To apply that scheme to the Lennard-Jones chains fluid model for $N>1$, we have considered that one molecule is one "particle" in the scaling procedure. Hence, in relation Eq. (19), N_p is equal to N_{mol} and $m=N\times M$, where M is the mass of the monomer.

Using that scaling on the LJC fluid model, the most striking result, as shown on Fig. 9, is that all reduced thermal conductivity values merge on the same "universal" curve whatever the chain length. Thus, it exists obviously a strong link between the reduced thermal conductivity and the reduced excess entropy of the LJC fluid model (at least for short chains). Concerning the validity of Eq. (20) on chains, it appears clearly on Fig. 10 that this relation is consistent only when restricted to a limited domain where roughly $-4<S^r<-1$.

2. Extension to low-density conditions

The approach proposed by Rosenfeld is based on a relation between thermal conductivity, adequately scaled, and the excess (configurational) part of the entropy. As shown in the previous section, such relation is not consistent in low density regime, i.e., when $S^r>-1$. This inconsistency is, among others, due to the fact that λ^r does not tend to zero when S^r tends to zero because of its dilute gas contribution. A similar inconsistency occurs when dealing with mass diffusion at low density [41]. So, we propose in this work to employ the "configurational" contribution to the thermal conductivity, i.e., the total thermal conductivity minus its dilute gas contribution, instead of using the total thermal conductivity in the scaling procedure, Eqs. (19) and (20). By doing so, we take advantage of the fact that the reduced configurational thermal conductivity tends to zero in the ideal gas limit ($S^r\to 0$).

As clearly shown on Fig. 11, this slightly modified scaling leads to a monotonic behavior of the reduced configurational thermal conductivity with the excess entropy even for $S^r>-1$ contrary to the classical scaling, see Figs. 8–10. Another very interesting feature of that modified scaling procedure is that the reduced configurational thermal conductivity of the LJC fluid model is roughly proportional to the reduced excess entropy for the whole range of thermodynamic conditions. More precisely a fitting indicates that using:

$$\lambda^r=\lambda_0^r-2.1S^r \tag{21}$$

it is possible to obtain a very reasonable estimation of the thermal conductivity of the LJC fluid model for all states and all chain lengths. Using Eq. (21) yields an AAD=18% with a MxD=43% compared to NEMD data over the whole range of thermodynamic states and chain length. This is reasonable

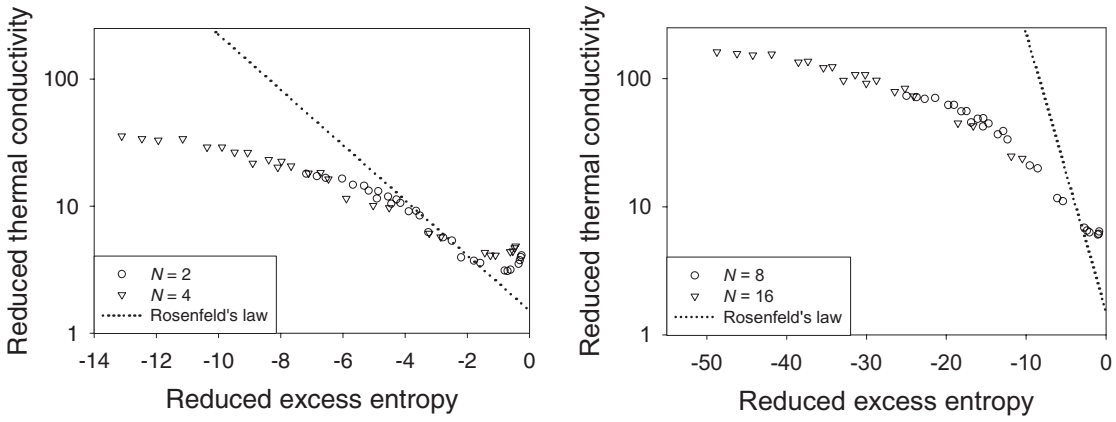

FIG. 10. Reduced thermal conductivity of LJ chains composed of N-mers computed by NEMD, plotted against reduced excess entropy calculated by the LJ-SAFT.

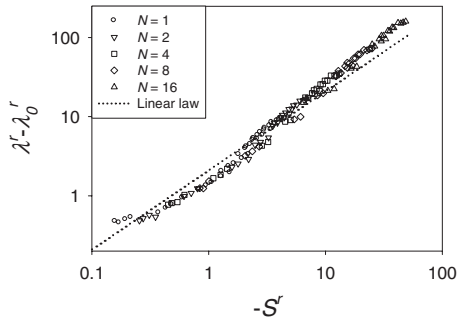

FIG. 11. Reduced "configurational" thermal conductivity of the LJC fluid against reduced excess entropy. The linear law corresponds to the plot of αS^r, with $\alpha=-2.1$, cf. Eq. (21).

taking into account the simplicity of the relation employed, Eq. (21), and the intrinsic errors on the data and on the estimation of the excess entropy.

IV. CONCLUSIONS

In this study, nonequilibrium molecular dynamics simulations have been performed to estimate, analyze and correlate the thermal conductivity of short Lennard-Jones chains ($N=1$, 2, 4, 8, and 16) for a large range of thermodynamic conditions.

For the Lennard-Jones fluid (monomer), it has been noticed that the value of the kinetic thermal conductivity, λ_k^*, deduced from NEMD simulations, coincides with the dilute gas value λ_0^* for sufficiently dilute conditions, i.e., when λ_k^*/λ^* is greater than 70%. So, using this approach, the values of the λ_0^* of the LJC fluid has been deduced from the computed λ_k^* for $N=2$, 4, and 8. As expected, due to the introduction of internal degrees of freedom, λ_0^* is decreasing with chain length. More precisely, it has been found that the dilute gas thermal conductivity of a LJ chain deduced from NEMD simulations is directly related to that of the monomer (the ratio between the two being equal to $(4N+11)/(15N^{3/2})$) in agreement with a model derived from the Eucken relation.

In dense states, NEMD simulation results indicate that the residual thermal conductivity, λ_r^*, of the LJ fluid (monomer) increases strongly with density, following $\ln(\lambda_r^*) \propto (\rho^*)^{1/2}$, but is weakly dependent on the temperature (a slight increase). Compared to the monomer value, it has been noted that the residual thermal conductivity of the LJC was slightly decreasing [proportionally to $(N-1)/N$] with the chain length.

Using all these results, we have proposed a simple correlation able to provide an accurate (AAD$<2.7\%$ and MxD$<6.75\%$) estimation of the thermal conductivity of the Lennard-Jones and Lennard-Jones chain fluid model (up to 16 segments) for the whole range of thermodynamic conditions studied, i.e., from $T^*=0.8$ to $T^*=6$ and up to $\rho^*=1$. It should be mentioned that this correlation, apart from the dilute gas and the residual contributions, contains a term related to the critical enhancement of the thermal conductivity. To estimate roughly this contribution (difficult to deal with using MD simulations), we have proposed a very simple scheme based on the computation of the isothermal compressibility thanks to a LJ-SAFT equation of state.

Additionally, we have analyzed the expected link between adequately reduced thermal conductivity, λ^r, and reduced excess entropy, S^r. It has been confirmed that the relation proposed by Rosenfeld, $\lambda^r=1.5e^{-0.5S^r}$, provides a semiquantitative estimation of the thermal conductivity only for $-4<S^r<-1$, i.e., mainly restricted to the LJ fluid from medium to high-density conditions. Very interestingly, it has been noted that all reduced thermal conductivity values merge on the same "universal" curve (function of S^r) whatever the chain length.

Finally, we have proposed a slight modification of the Rosenfeld's approach to extend it toward low density conditions. To do so, we employ the configurational contribution to the thermal conductivity (the total thermal conductivity minus its dilute gas contribution) instead of using the total thermal conductivity in the scaling procedure. This approach ensures a value equal to zero when S^r tends to zero, contrary to the original scheme. Using this modification, it is shown that the reduced configurational thermal conduction of the LJC fluid model is approximately proportional to S^r for all states and all chain lengths.

ACKNOWLEDGMENTS

We gratefully acknowledge computational facilities provided by the UPPA and the TREFLE laboratory, which supercomputer has been financially supported by the Conseil Régional d'Aquitaine. This work has been partly supported by the DSC program managed by the ESA.

[1] S. Chapman and T. G. Cowling, *The Mathematical Theory of Non-Uniform Gases* (Cambridge Mathematical Library, Cambridge, 1970).
[2] M. J. Assael, J. P. M. Trusler, and T. F. Tsolakis, *Thermophysical Properties of Fluids* (Imperial College Press, London, 1996).
[3] B. E. Poling, J. M. Prausnitz, and J. P. O'Connell, *The Properties of Gases and Liquids* (McGraw-Hill, New York, 2001).
[4] H. Sigurgeirsson and D. M. Heyes, Mol. Phys. **101**, 469 (2003).
[5] D. D. Royal, V. Vesovic, J. P. M. Trusler, and W. A. Wakeham, Mol. Phys. **101**, 339 (2003).
[6] D. M. Heyes and A. C. Branka, Phys. Chem. Chem. Phys. **7**, 1220 (2005).
[7] R. L. Rowley and M. M. Painter, Int. J. Thermophys. **18**, 1109 (1997).
[8] J. H. Dymond, Int. J. Thermophys. **18**, 303 (1997).
[9] G. Galliéro, C. Boned, and A. Baylaucq, Ind. Eng. Chem. Res.

44, 6963 (2005).
[10] R. Laghaei, A. E. Nasrabad, and B. C. Eu, J. Chem. Phys. **123**, 234507 (2005).
[11] A. S. De Wijn, V. Vesovic, G. Jackson, and J. P. M. Trusler, J. Chem. Phys. **128**, 204901 (2008).
[12] O. Suarez-Iglesias, I. Medina, C. Pizarro, and J. L. Bueno, Chem. Eng. Sci. **62**, 6499 (2007).
[13] G. Galliero and C. Boned, Phys. Rev. E **79**, 021201 (2009).
[14] M. J. Assael, Int. J. Thermophys. **13**, 269 (1992).
[15] R. Laghaei, A. E. Nasrabad, and B. C. Eu, J. Chem. Phys. **124**, 084506 (2006).
[16] M. Bugel and G. Galliero, Chem. Phys. **352**, 249 (2008).
[17] Y. Rosenfeld, Phys. Rev. A **15**, 2545 (1977).
[18] R. Grover, W. G. Hoover, and B. Moran, J. Chem. Phys. **83**, 1255 (1985).
[19] H. C. Andersen, J. Comput. Phys. **52**, 24 (1983).
[20] F. Müller-Plathe, J. Chem. Phys. **106**, 6082 (1997).
[21] D. Bedrov and G. D. Smith, J. Chem. Phys. **113**, 8080 (2000).
[22] B. Hafskjold, T. Ikeshoji, and S. K. Ratkje, Mol. Phys. **80**, 1389 (1993).
[23] R. D. Mountain, J. Chem. Phys. **124**, 104109 (2006).
[24] M. P. Allen and D. J. Tildesley, *Computer Simulations of Liquids* (Oxford Science Publications, Oxford, 1987).
[25] H. J. C. Berendsen *et al.*, J. Chem. Phys. **81**, 3684 (1984).
[26] D. F. Botelho, P. S. Branicio, and J. P. Rino, Diffus. Defect Data, Pt. A **258**, 310 (2006).
[27] P. D. Neufeld, A. R. Janzen, and R. A. Aziz, J. Chem. Phys. **57**, 1100 (1972).
[28] B. D. Todd, P. J. Daivis, and D. J. Evans, Phys. Rev. E **51**, 4362 (1995).
[29] D. K. Dysthe, A. H. Fuchs, and B. Rousseau, J. Chem. Phys. **110**, 4047 (1999).
[30] M. H. Ernst, E. H. Hauge, and J. M. J. Leeuwen, J. Stat. Phys. **15**, 7 (1976).
[31] K. Meier, *Computer Simulation and Interpretation of the Transport Coefficients of the Lennard-Jones Model Fluid* (Shaker Publishers, Aachen, 2002).
[32] J. V. Sengers, Int. J. Thermophys. **6**, 203 (1985).
[33] D. J. Searles, *et al.*, Mol. Simul. **20**, 385 (1998).
[34] P. M. Mathias, V. S. Parekh, and E. J. Miller, Ind. Eng. Chem. Res. **41**, 989 (2002).
[35] J. Kolafa and I. Nezbeda, Fluid Phase Equilib. **100**, 1 (1994).
[36] D. O. Dunikov, S. P. Malyshenko, and V. V. Zhakhovskii, J. Chem. Phys. **115**, 6623 (2001).
[37] J. K. Johnson, E. A. Müller, and K. E. Gubbins, J. Phys. Chem. **98**, 6413 (1994).
[38] R. Holmen, M. Lamvik, and O. Melhus, Int. J. Thermophys. **23**, 27 (2002).
[39] M. Dzugutov, Nature (London) **381**, 137 (1996).
[40] Y. Rosenfeld, J. Phys.: Condens. Matter **11**, 5415 (1999).
[41] S. Bastea, Phys. Rev. E **68**, 031204 (2003).
[42] E. H. Abramson and H. West-Foyle, Phys. Rev. E **77**, 041202 (2008).
[43] T. Goel, C. N. Patra, T. Mukherjee, and C. Chakravarty, J. Chem. Phys. **129**, 164904 (2008).